

OMAE2009-80069

HIGHER ORDER RESONANT INTERACTION OF SURFACE WAVES BY UNDULATORY BOTTOM TOPOGRAPHY

Mohammad-Reza Alam

Department of Mechanical Engineering
Massachusetts Institute of Technology
Cambridge, Massachusetts, 02139
Email: alam@mit.edu

Yuming Liu

Department of Mechanical Engineering
Massachusetts Institute of Technology
Cambridge, Massachusetts, 02139
Email: yuming@mit.edu

Dick K.P. Yue

Department of Mechanical Engineering
Massachusetts Institute of Technology
Cambridge, Massachusetts, 02139
Email: yue@mit.edu

ABSTRACT

Higher order (quartet) Bragg resonance of water waves by bottom undulations and its effect on the evolution of ocean wave spectrum, particularly over continental shelves and littoral zones, are considered. Higher order Bragg resonance can provide a viable mechanism for distribution of (initially confined) energy across the spectrum. Contrary to classical Bragg resonances (Class I and II) where the resonant wave has to have the same frequency as the incident wave, Class III (quartet) Bragg resonance of three free waves and a bottom topography component allow participant waves to have different frequencies. Of particular interest here are higher-order resonances that lead to infragravity wave generation as a result of interaction of regular sea waves with bottom undulations (of the same order of wavelength as the primary waves), and, long/medium surface wave generation by nonlinear interaction between short surface waves and medium wavelength bottom undulations. These mechanisms can accelerate the rate by which energy is damped by the bottom friction. The second mechanism also provides a potential alternative mechanism for explaining microseismic noise observed in shallow waters. We further consider the oblique higher order Bragg resonance. Although for Class I, oblique resonance is less important than normal incidence, it is shown here via illustrative examples and direct simulations that there are strong oblique Class II and III Bragg cases. Inclusion of higher order interactions paves a path for the energy transfer to higher and lower frequencies of an initially narrow band spectrum. Ensuing multiple (exact/near) such resonant interactions can result in the generation of multiple new transmitted/reflected waves that fill a

broad wavenumber band eventually leading to loss of order and chaotic motion of water surface.

INTRODUCTION

We consider the higher order resonant interactions of surface waves travelling over bottom undulations. The problem is similar to the second order case, in that waves are modified, i.e., exchange energy, as they travel over and interact with the nonuniform bottom topography. In higher order, however, unlike the second order, Bragg resonance can occur between waves of different frequencies. This fact suggests the possibility of generation of resonant waves with (much) higher and lower frequencies than the initial waves. Furthermore, when an incident wave traveling over the rippled region satisfies the higher order Bragg condition the resonant wave can be a reflected or transmitted wave. Bragg resonance can affect the development of the wave spectrum in the coastal regions and continental shelves (e.g. 1; 2; 3; 4), modify the shore-parallel sandbars (e.g. 5), result in new wave formations that are of concern to, for example, ocean vehicles moored in shallow basins (e.g. 6) and affect the micro-seismic spectrum (e.g. 7) in places where bottom topography variation is appreciable.

The second order interaction of surface waves with bottom undulations has been studied extensively, owing to its importance in the formation of near-shore sandbars and the evolution of ocean wave-field in littoral zones. Regular perturbation analysis has been invoked to find the amplitude growth rate of the resonant wave at and near the resonance (8). The result of this ap-

proach becomes unbounded when the number of bottom ripples increases indefinitely. To overcome this, multiple-scale analysis offers a formulation that derives a uniformly convergent solution for the interacting wave components (1). A similar result can be obtained by extending the mild slope equation to include the effect of fast bottom undulations (9). By including higher-order interactions, in (10) second-order Bragg resonance is generalized to include third-order quartet resonant interactions of waves and bottom ripples, but only equi-frequency cases are considered.

Ocean generated noise contributes to the mid-frequency region of micro-seismic spectrum (7). The spectrum has two clearly distinguishable peaks, at periods of about $T_1=14$ sec (primary, 12-18 sec) and $T_2=7$ sec (secondary, 6-9 sec), whose source is yet unclear(11). Primary micro-seisms were recorded at north German coast and north Swedish station (Umea) coming from the entire north Norwegian coast, and secondary at northern Scandinavia, Norwegian coast, North Channel and the Bristol Channel (11). Ocean generated micro-seisms were originally attributed to ocean swell, and a better understanding was provided when (12) showed how nonlinear wave-wave resonance can generate waves of half period. However, Observations of (11) suggest that the secondary micro-seismic wavefield is not due to wave-wave interactions near/at the storm center, but is possibly due to the interaction of incident waves and *local geometrical structures*. It is further conjectured that the transfer of ocean storm energy to infragravity waves facilitates the wave-bottom interactions, resulting in stronger micro-seismic signals from certain geographical locations (13; 14).

Higher order wave interactions in the ocean and the generation of new frequency resonant wave are of importance, also, to the loading conditions of moored ships. Loading and off-loading subject a ship to a regular change of its weight and depth to draft ratio, resulting in the variation of its natural frequency and hydrodynamic properties (15; 16). Therefore even low amplitude waves at specific range of frequencies may result in a drastic motion of the ship, as is a concern for moored LNG carriers in shallow basins where such motions are synonymous with the strong internal sloshing if the tank is not fully filled (6). Bottom Topography is already known to be a determining factor for the direction of dominant waves in such basins, and here we show its potential effect in disturbing the wave field by generating resonant waves.

Although the formulation of higher order Bragg resonance has been obtained in principle (e.g. 3), or has been given in some special cases (10), resonance possibilities have not been worked out. Here we show a more general geometric construction for different classes of Bragg resonance and via illustrative examples supported by direct simulations show how higher order resonance can result in appreciable unexpected waves. These results may have direct implications in a safer design of offshore structures, more accurate estimations of the work condition of moored ships in shallow basins, and better understanding of ocean wave

spectrum in shallow waters with a rough bottom.

Problem definition is given in §1, followed by a discussion on the Bragg resonance condition and geometric construction at the second and the third order in §2. In §3 a selection of relevant examples are presented and discussed. It is shown, for example, that regular sea waves can generate infragravity waves as a result of high order interaction with typical near shore sandbars. The case of oblique resonance is much richer in terms of numbers and types of possible resonances. For example it is shown that starting from a single monochromatic incident wave, higher order resonance can result in an accurate symmetric three dimensional standing wave in a finite time. This may have implications in three dimensional wave generation in towing tanks with one wave generating paddle.

1 Problem Formulation

We consider a potential flow with incident wave(s) propagating over non-uniform bottom topography, subject to the condition of relatively mild surface/interface/bottom wave slopes. Of basic interests here are the conditions involving the incident wave and bottom topology wavenumbers for a given water depth for which (generalized) Bragg resonant interactions obtain.

We define a cartesian coordinate system with x -axis on the mean free surface and z -axis positive upward. We consider a fluid of depth h and density ρ resting on a rippled horizontal bottom given by $z = -h + \eta_b$ where η_b is the elevation of the bottom undulation measured from the mean bottom depth. We assume that the fluid is homogeneous, incompressible, immiscible and inviscid so that the fluid motion is irrotational. The effect of surface tension is neglected. The flow is described by a velocity potential, $\phi(\mathbf{x}, z, t)$. The exact nonlinear equations read:

$$\nabla^2 \phi + \phi_{zz} = 0 \quad -h + \eta_b < z < \eta_s \quad (1.1a)$$

$$\phi_{tt} + g\phi_z + (\partial_t + 1/2 \nabla \phi \cdot \nabla + 1/2 \phi_z \partial_z) (|\nabla \phi|^2 + \phi_z^2) = 0 \quad z = \eta_s \quad (1.1b)$$

$$g\eta_s + \phi_t + 1/2 (|\nabla \phi|^2 + \phi_z^2) = 0 \quad z = \eta_s \quad (1.1c)$$

$$\nabla \phi \cdot \nabla \eta_b - \phi_z = 0 \quad z = -h + \eta_b \quad (1.1d)$$

where $\nabla = (\partial_x, \partial_y)$, $\eta_s(\mathbf{x}, t)$ is the elevations of the free-surface and g is the gravity acceleration.

For small surface waves over a mildly varying bottom topography η_b , we expand the velocity potential (ϕ) in perturbation series with respect to a small parameter ϵ that measures the wave/bottom steepnesses which are assumed, for simplicity, to be of the same order:

$$\phi = \epsilon \phi^{(1)} + \epsilon^2 \phi^{(2)} + O(\epsilon^3). \quad (1.2)$$

Substituting (1.2) into (1.1), expanding the quantities on the free

surface and bottom in Taylor series with respect to the respective mean positions, different order equations are obtained by collecting terms at each order $m = 1, 2, \dots$. In a regular perturbation approach, at each order, a system of linear equations (with all possibly lower order nonlinearities moved to the right-hand side) are solved successively to higher order starting from $m=1$.

At $m=1$, the set of governing equations is homogeneous, and the eigen solution representing a free propagating wave can be written as

$$\phi^{(1)} = A \cos(\mathbf{k}\mathbf{x} - \omega t), \quad (1.3)$$

where ω and \mathbf{k} represent the frequency and wavenumber of the wave respectively, and satisfy the dispersion relation:

$$\mathcal{D}(\mathbf{k}, \omega) \equiv \omega^2 - gk \tanh kh = 0, \quad (1.4)$$

where $k = |\mathbf{k}|$.

2 Bragg resonances

Consider a right-going incident wave of frequency ω , wavenumber \mathbf{k} and amplitude a propagating over a rippled bottom with the elevation given by

$$\eta_b(\mathbf{x}) = d \sin(\mathbf{k}_b \cdot \mathbf{x}) \quad (2.5)$$

where d and \mathbf{k}_b are respectively the amplitude and wavenumber of the bottom undulations. At the second order ($m = 2$), if $\mathbf{k} \pm \mathbf{k}_b$ and ω satisfy the dispersion relation, i.e.,

$$\left. \begin{array}{l} \mathcal{D}(\mathbf{k}_r, \omega) = 0 \\ \mathbf{k}_r = \mathbf{k} \pm \mathbf{k}_b \end{array} \right\}, \quad (2.6)$$

where the subscript r denotes the resonant wave, the interaction term is secular and the second-order interaction becomes resonant. As a result, a free propagating wave of wavenumber \mathbf{k}_r and frequency ω is generated. The initial growth of the resonant wave amplitude a_r is given by:

$$a_r \propto a d t \quad (2.7)$$

for a long uniformly-rippled bottom. Under this condition, (2.7) shows that the amplitude of the generated wave grows indefinitely over time. Equation (2.6) is called the class I Bragg condition. Figure 1.a shows a geometric construction of class I triad. Without loss of generality we assume that the incident wave \mathbf{k}_1

moves along positive x -axis. Now a bottom topography with wavenumber \mathbf{k}_b can resonate another free surface wave \mathbf{k}_r , with the same frequency as that of the incident wave, if it connects the end of \mathbf{k}_r arrow to another point on the circle with radius $r = |\mathbf{k}|$. This circle is in fact a horizontal cross section of three dimensional cone-shape dispersion relation at a given frequency ω . This geometric construction in fact gives the same result as of (10). Class I Bragg resonance has been studied extensively: regular perturbation technique (8), multiple scales (1), mild slope equation (9), numerical validation (10) and with a more complicated incident wave field (17).

The resonance interactions occur also at third-order ($m=3$) involving quartets of propagating/bottom modes. These belong to two broad types: one consisting of two free wave and two bottom ripple components; and the other three wave components and one bottom component. The resonance associated with the former/latter quartet wave-bottom interaction is denoted as class II/III Bragg resonance.

To illustrate the class II Bragg resonance condition, we consider a bottom elevation which is given by the superposition of two ripple components of wavenumbers k_{b1} and k_{b2} . Upon carrying out the perturbation analysis to the third order it turns out that the bottom forcing contains terms proportional to $\sin[(\mathbf{k} \pm 2\mathbf{k}_{b1})x - \omega t]$, $\sin[(\mathbf{k} \pm 2\mathbf{k}_{b2})x - \omega t]$, and $\sin[(\mathbf{k} \pm \mathbf{k}_{b1} \pm \mathbf{k}_{b2})x - \omega t]$. Class II Bragg resonance occurs whenever the wavenumber $\mathbf{k} - 2\mathbf{k}_{b1}$ or $\mathbf{k} \pm 2\mathbf{k}_{b2}$ or $\mathbf{k} \pm \mathbf{k}_{b1} \pm \mathbf{k}_{b2}$ and the frequency ω satisfy the dispersion relation (1.4). Thus, in general form, the class II Bragg resonance condition can be expressed as:

$$\left. \begin{array}{l} \mathcal{D}(\mathbf{k}_r, \omega) = 0 \\ \mathbf{k}_r = \mathbf{k} \pm \mathbf{k}_{b1} \pm \mathbf{k}_{b2} \end{array} \right\}. \quad (2.8)$$

The class II resonance condition (2.8) is identical to the class I resonance condition (2.6) if k_b in (2.6) is replaced by the super- or sub-harmonic combination of the two bottom ripple components $\mathbf{k}_{b1} \pm \mathbf{k}_{b2}$. Class II resonance is thus a direct extension of class I resonance to the third order. Similarly the geometric construction of class II is similar to class I with \mathbf{k}_b vector being replaced by $\mathbf{k}_{b1} \pm \mathbf{k}_{b2}$, and is shown in figure 1-b.

In class III Bragg resonance, the resonant quartet is composed of three travelling waves and one bottom ripple component. To obtain this resonance condition, we consider the general case involving two incident waves of wavenumbers, \mathbf{k}_1 and \mathbf{k}_2 , and frequencies, ω_1 and ω_2 . Without loss of generality, we assume $k_1 > |k_2| > 0$. Starting with the linear solution for the two free wave components and carrying out the perturbation analysis to the third order, the inhomogeneous terms contain expressions proportional to $\sin[(2\mathbf{k}_1 \pm \mathbf{k}_b)x - 2\omega_1 t]$, $\sin[(2\mathbf{k}_2 \pm \mathbf{k}_b)x - 2\omega_2 t]$, and $\sin[(\mathbf{k}_1 \pm \mathbf{k}_2 \pm \mathbf{k}_b)x - (\omega_1 \pm \omega_2)t]$. If the combined wavenumber and frequency in any of these forcing terms satisfy the dis-

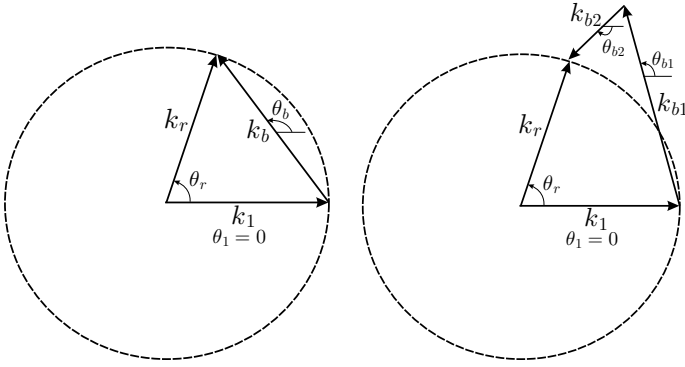


Figure 1. Geometric construction of the a) class I triad and b) class II quartet Bragg resonant waves. Wave k_1 is assumed to move along the positive x -axis.

persion relation, the associated wave-bottom interaction becomes resonant and a third free wave component is generated by the resonance. The condition for class III Bragg resonance can be written in the following general form:

$$\left. \begin{array}{l} \mathcal{D}(\mathbf{k}_r, \omega_r) = 0 \\ \mathbf{k}_r = \mathbf{k}_1 \pm \mathbf{k}_2 \pm \mathbf{k}_b, \quad \omega_r = \omega_1 \pm \omega_2 \end{array} \right\} \quad (2.9)$$

in which \mathbf{k}_r and ω_r represent the wavenumber and frequency of the resonant generated wave.

Due to the involvement of three free propagating waves, combinations of wave components in class III resonance are more complicated than those in class II resonance. Graphical constructions similar to those of figure 1 can be formed for class III Bragg resonance in a general finite depth case for a) subcritical (i.e. $\omega_r = \omega_1 - \omega_2$) and b) supercritical (i.e. $\omega_r = \omega_1 + \omega_2$) cases, which for the interest of space are not shown here. In a subcritical case, for a given \mathbf{k}_1 and \mathbf{k}_2 (without loss of generality we assume $\mathbf{k}_1 = k_1 \hat{i}$ and $k_1 = |\mathbf{k}_1| > |\mathbf{k}_2|$), a bottom component \mathbf{k}_b that connects the end of the arrow $\mathbf{k}_1 + \mathbf{k}_b$ to the resonance circle forms a quartet class III Bragg resonance. The resonance circle is a circle centered at the origin and with radius $r = k_r = |\mathbf{k}_r|$ where k_r is the solution to the equation $\mathcal{D}(\mathbf{k}_r, \omega_r) = 0$ with $\omega_r = \omega_1 - \omega_2$. The resonance circle never crosses the \mathbf{k}_2 side circle (with radius $r = |\mathbf{k}_2|$), i.e. $\omega_r < \omega_1 - \omega_2$. Note that since θ_b and $\pi + \theta_b$ form the same bottom topography, the $\theta_b < \pi$ always chosen for the definition of the bottom wavenumber angle. In the case of superharmonic class III Bragg resonance, the resonance circle is always outside \mathbf{k}_2 circle. A similar discussion as for subcritical case applies here for the geometric construction.

3 Results

In this section a number of representative higher order Bragg resonance is considered and potential applications are discussed.

In a two dimensional configuration, higher order (class III) Bragg resonance can contribute to resonant waves with possibly comparable amplitude to the original (incident) waves. In the presence of regular seabed undulations, i.e. $O(10 - 100)\text{m}$ (see e.g. 18), co-propagating short surface waves can resonate regular surface waves for example, and counter-propagating regular surface waves can resonate infragravity waves. We further consider oblique cases when the possibility of resonance cases is much higher. It is shown that higher order resonance, via a biharmonic topography, can distribute the energy of a monochromatic incident surface wave equally in four waves (including the incident wave itself) resulting in a symmetric three dimensional standing wave on the water surface. Two examples of class III Bragg resonance are also discussed where a subharmonic long cross-wave is generated when two co-propagating surface waves travel on an oblique undulatory region, and, when two co-propagating surface waves travel over a perpendicular bottom topography form two (superharmonic) oblique surface waves which are symmetric with respect to the direction of incident waves, and hence form a moving egg-rack pattern on top of initial incident waves. Numerical simulations are performed by a Higher Order Spectral (HOS) method (see 10).

3.1 Two dimensional higher order Bragg resonance

Two dimensional class III Bragg resonance, when incident waves have non-equal frequencies, offers a viable mechanism for the generation of a variety of new frequencies that originally do not exist in the spectrum. Here we consider two cases of this kind and show that, via numerical simulations, the amplitude of the resonant generated wave can be comparable to the initial incident waves.

Case 1. Resonance of a subharmonic regular surface wave by two co-moving short surface waves traveling over a regular bottom undulation. To illustrate this case consider, for example, $\lambda_1 = 10\text{ m}$ and $\lambda_2 = 15\text{ m}$ co-propagating surface waves in a shallow basin of $h = 5\text{ meters}$, carpeted with a topography of dominant wavelength of $\lambda_b = 44\text{ m}$, which can excite a $\lambda_r = 86\text{ meter}$ surface wave.

To numerically show the strength of this resonance, consider a long 2D basin such that all $\partial/\partial x = 0$. To simulate wave interaction over such a basin, we consider a finite length of this basin $L = 20\lambda_r$ and apply periodic boundary condition at both ends at $x = 0$ and $x = 20\lambda_r$. Initial wave amplitudes are respectively $a_1 = 14\text{ cm}$ and $a_2 = 7\text{ cm}$ for wave 1 and 2. To nondimensionalize we take a length scale of $L_0 = 274\text{m}$ such that the taken portion is mapped to $0 < \bar{x} < 2\pi$. Time scale is chosen such that $gT_0^2/L_0 = 1$.

Figure 3-a shows numerical simulation of this case for a time period of $0 < t/T_0 < 450$. At the cost of decrease in the amplitude of wave k_1 , the amplitudes of resonant wave k_r and wave k_2 initially increase with time. The resonance growth is strong enough

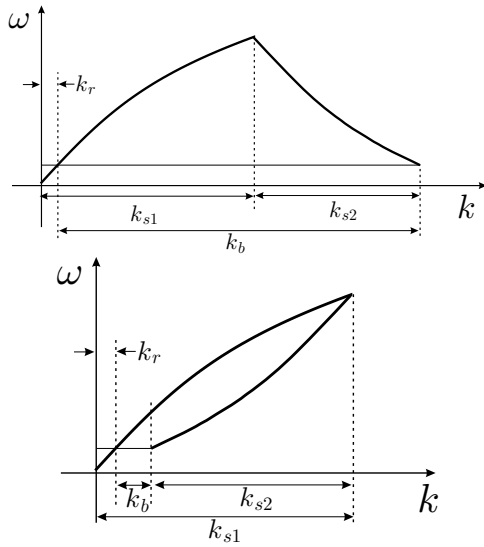


Figure 2. Schematic of the dispersion relationship for a. Infragravity resonant wave generation as a quarter resonance between two regular surface waves and a bottom undulation with a wavenumber of the same order as that of surface waves (almost half), and, b. regular surface wave generation as a result of quartet Bragg resonance between two very short surface waves and a monochromatic bottom undulation of regular wave length.

such that the amplitude of the resonant wave becomes comparable to the initial surface waves. If the simulation runs for long enough time, the direction of energy propagation reverses and the energy moves back, from resonant wave k_r and wave k_2 , to the wave k_1 . Modulation in time has to continue should there be no other interactions. However, due to the other leading/higher order exact/near resonances, energy disperses over the spectrum after a while.

Case 2. Resonance of an infragravity surface wave by two heading regular surface waves traveling over a regular bottom undulation. For example $\lambda_1=80$ m and $\lambda_2=132$ m oppositely-propagating surface waves in a shallow basin of $h=50$ meters carpeted with a topography of dominant wavelength of $\lambda_b=54$ m can excite a $\lambda_r=672$ meter surface wave.

Similar to case 1, we pick a long basin such that $\partial/\partial x = 0$ with length $L = 20\lambda_r$. Initial wave amplitudes are respectively $a_1 = 1$ m and $a_2=2$ m. Nondimensionalizing scales are $L_0 = 2140$ m and $T_0=0.485$ sec. Figure 3-b shows the modulation of the initial wave and resonant wave amplitudes. The weaker growth in this case (compared to the case in figure 3-a) is partially due the assumption of 10 times deeper water. Nevertheless the short amplitude resonance generated infragravity wave with the period of $T \approx 30$ seconds is long enough to be able to resonate LNG tankers.

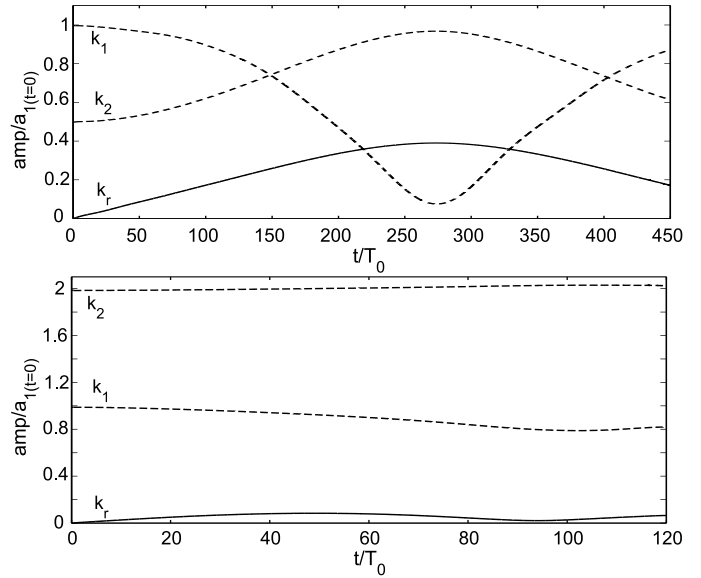


Figure 3. Evolution of amplitudes of incident and resonant waves in two-dimensional Class III Bragg resonance: a) Example 1 and b) Example 2.

3.2 Symmetric three-dimensional standing wave generation by class II

A symmetric three-dimensional standing wave is generated when two perpendicular standing wave with no (or π) phase difference are superimposed on top of each other. Here we show that class II Bragg resonance can be used to generate an almost perfect such wave starting with only one monochromatic incident surface wave $\mathbf{k} = k\hat{i}$.

For this purpose, assume a bottom topography with two components $\mathbf{k}_{b1}=(k,0)$ and $\mathbf{k}_{b2}=(0,k)$. The first bottom topography \mathbf{k}_{b1} at the third order, when being counted two times, reflects a part of the energy of incident wave \mathbf{k}_1 and forms a two dimensional standing wave with crests parallel to the y -axis. However, $\mathbf{k}_1 - \mathbf{k}_{b1} + \mathbf{k}_{b2}=(0,k)=\mathbf{k}_r^+$ satisfies the dispersion relation (i.e. $\mathcal{D}(\omega, k_r^+) = 0$), and hence is a resonant wave and will be formed. Interestingly, a similar wave but with opposite direction of propagation is also a resonant wave in this system: $\mathbf{k}_r^-=\mathbf{k}_1 - \mathbf{k}_{b1} - \mathbf{k}_{b2}=(0,-k)$. Due to the symmetry the energy sinks from the incident wave equally into waves \mathbf{k}_r^+ and \mathbf{k}_r^- which will form a standing wave with crests parallel to x -axis. If the resonance is strong enough, and the phase matching occurs, at a certain time the amplitude of both sets of standing waves are equal, and a symmetric three dimensional standing wave appears on the surface.

To numerically show this possibility, we consider a monochromatic incident surface wave of normalized wavenumber $\mathbf{k}=(5,0)$ with a bottom composed of $\mathbf{k}_{b1}=(5,0)$ and $\mathbf{k}_{b2}=(0,5)$ in a shallow basin of normalized depth $h = 0.1257$. Numeri-

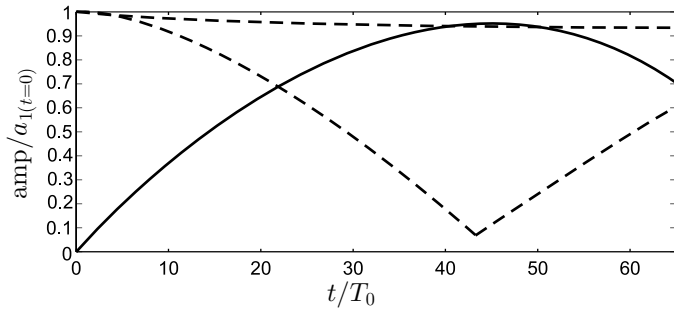


Figure 4. Growth of the amplitude of the resonant standing wave (solid line) and the decay in the amplitude of the incident wave (dash-lines) as the standing waves are being formed.

cal simulation shows (figure 4) that after a time about $t \approx 45T_0$, where T_0 is the period of the incident wave, the amplitudes of x -parallel and y -parallel standing waves are close. The graph is generated by measuring the (spatial) Fourier components of the wave field. If waves are progressive, the corresponding Fourier amplitude stays constant as long as the amplitude is constant. If standing, then the corresponding Fourier amplitude oscillates. The solid line in figure 4 is a push (Hilbert transform) to the curve corresponds to the resonant wave. The dash-lines are upper and lower pushes for the incident wave. Note that at the beginning the incident wave is a simple monochromatic progressive wave, hence no oscillation is seen in the Fourier amplitude. As the reflected wave forms (i.e. standing wave starts to form), the Fourier amplitude starts to oscillate and lower dash-line curve has to be introduced.

The three dimensional standing wave pattern at the peak of the amplitude of the resonant wave (i.e. $t \approx 45T_0$) is shown in figure 5. This mechanism can be used in experimentations in towing tanks with one paddle to form symmetric (or different) standing waves and offers another potential mechanism for the generation of standing waves in shallow basins that may help better understanding of the micro-seismic spectrum.

3.3 Oblique class III Bragg resonance

Oblique class III Bragg resonance can significantly affect the evolution of ocean spectrum, and contribute to the generation of new frequency waves. This is of importance in many practical applications including the operation of large LNG carriers offshore, yet close to harbors, where the water is shallow and waves are multi-directional (6).

As an illustrative example here we consider a case in which, due to class III Bragg resonance, a resonant wave forms with its direction of propagation perpendicular to the direction of the original co-propagating uni-directional incident waves.

Consider $\lambda_1=10$ m and $\lambda_2=18.7$ m co-propagating surface waves propagating along the positive x -axis in a very shallow

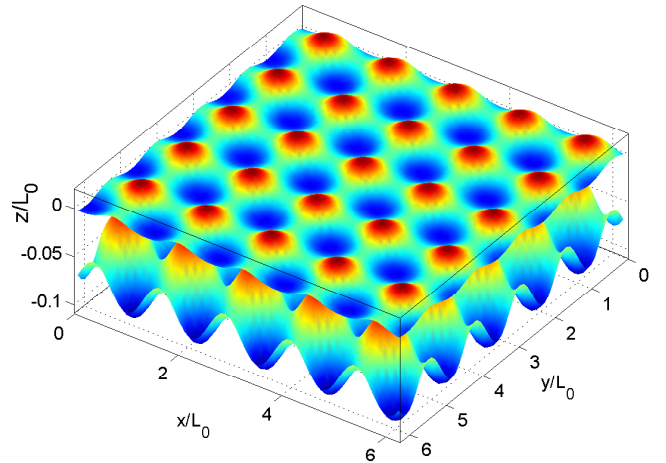


Figure 5. A symmetric standing wave pattern formation as a result of third order Bragg resonance of a monochromatic incident wave with two bottom topography components.

basin of $h = 2$ meters depth. If the topography wavelength is $\lambda_b=75$ m and its wavenumber makes $\theta_b = 35$ degree with the positive x -axis, a relatively long (subharmonic) surface wave of $\lambda_r=30$ m propagating perpendicularly to the initial surface waves will be generated as a result of oblique class III Bragg resonance between waves of different frequencies.

To simulate this problem, we take normalized variables $L_0=24$ m for length and $T_0=1.57$ sec for time. Numbers of points along x - and y -axis are $NDX=128$ and $NDY=64$ respectively, and $\delta t/T_1=32$ where T_1 is the period of the first incident surface wave. Figure 6 compares the surface pattern in a linear simulation with the simulation in which nonlinearities are taken into account (order of nonlinearity in HOS is set to $M=4$). Cross-waves with wavenumber $k_r = 5$ are clearly seen, perpendicular to the crests of the initial incident waves. Figure 7 shows the measured amplitude as a function of time.

Superharmonic class III Bragg resonance happens when the frequency of the resonant wave is the sum of frequencies of incident waves. Consider two incident waves of wavenumbers $\mathbf{k}_1, \mathbf{k}_2$ and a topography with the wavenumber \mathbf{k}_b . Assume $\mathbf{k}_r^+ = \mathbf{k}_1 + \mathbf{k}_2 + \mathbf{k}_b$ is a resonant wave, i.e. $\mathcal{D}(\mathbf{k}_r^+, \omega_r) = 0$ where $\omega_r = \omega_1 + \omega_2$. Now if $\mathbf{k}_b \perp (\mathbf{k}_1 + \mathbf{k}_2)$, then $\mathbf{k}_r^- = \mathbf{k}_1 + \mathbf{k}_2 - \mathbf{k}_b$ has to be a resonant wave too. In a special case when \mathbf{k}_1 and \mathbf{k}_2 are aligned, there is no preferred direction, hence energy has to be equally distributed between \mathbf{k}_r^+ and \mathbf{k}_r^- resulting in a propagating pattern in the direction parallel to $(\mathbf{k}_1 + \mathbf{k}_2)$ and a standing pattern in the perpendicular direction. The 3D pattern propagation then looks like a moving egg-rack.

As an example consider two incident wave with normalized wavenumbers $\mathbf{k}_1=(8,0)$ and $\mathbf{k}_2=(5,0)$ traveling over bottom un-

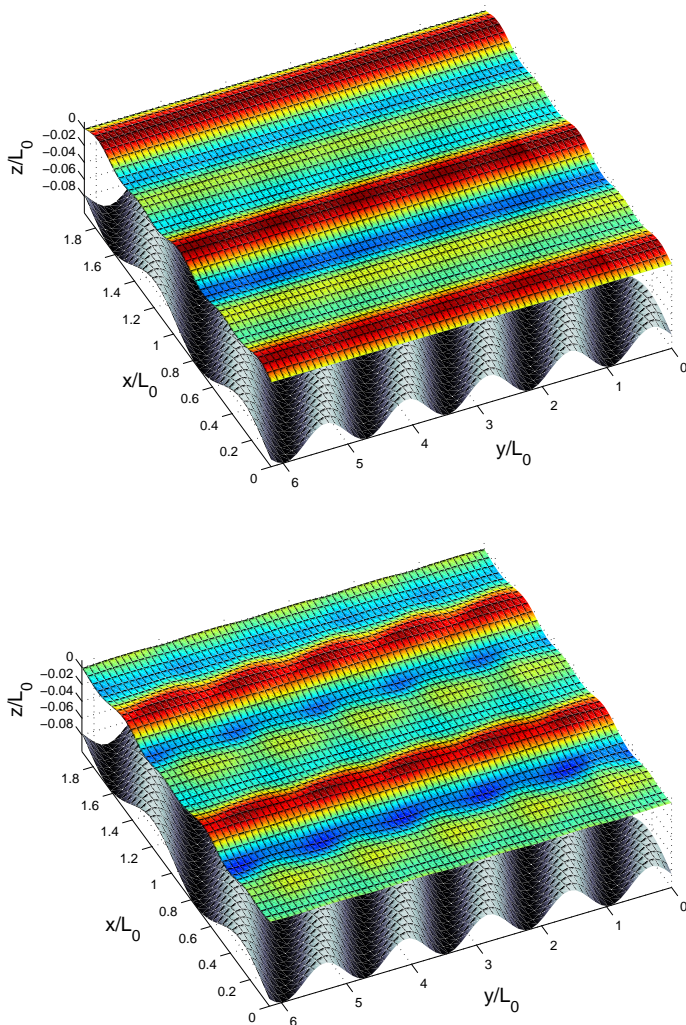


Figure 6. High order numerical simulation of waves propagating over undulatory topography when class III Bragg resonance condition is satisfied. a. Linear simulation b. higher order simulation. Cross waves $k_b=5$ are observed perpendicular to the direction of propagation of incident waves.

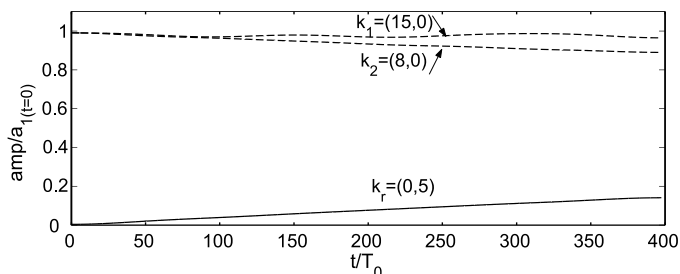


Figure 7. Evolution of amplitudes of incident and resonant waves in an oblique class III Bragg resonance. Normalized wave numbers are shown on the figure.

dulation with perpendicular wavenumber of $\mathbf{k}_b=(0, 12)$ in a water of normalized depth $h=0.1257$. In a sea of depth 10 m, these numbers correspond to waves with wavenumbers $\lambda_1=100$ m and $\lambda_2=62.5$ m with a bottom wavelength of $\lambda_b=42$ m. These two incident waves and bottom component satisfy the superharmonic class III Bragg resonance and since $\mathbf{k}_b \perp (\mathbf{k}_1 + \mathbf{k}_2)$ a double class III Bragg resonance happens.

Figure 8 shows a numerical simulation of this case. Number of points along x - and y -axis are $NDX=128$ and $NDY=64$ respectively, and $\delta t/T_1=16$ where T_1 is the period of the first incident surface wave. Figure 8a shows the surface pattern if no nonlinearity is taken into account whereas taking higher order ($M=4$) nonlinearity results in the generation of relatively strong oblique waves superimposed on the surface. The oblique resonant wave growth as a function of time is shown in figure 9 where due to the amplitude decay of initial surface waves the new resonant wave arises. However, the crests of the resonant oblique waves do not move in the y -direction. This can be seen from figure 10 where a top view of the wavefield is depicted for two relatively close times. With waves propagating in the x -direction clearly observed, the crests in the y -direction are stationary.

4 Conclusion

Higher order oblique and normal resonance interaction of surface waves with bottom topography is considered and a number of potential applications is underscored via illustrative examples and direct numerical simulations. At the third order, two surface waves can be in resonance via two bottom components (Class II Bragg resonance), or, three surface waves via one bottom component (Class III Bragg resonance). Contrary to Class I and II, where participating waves in a triad/quartet resonance have the same frequency, in Class III they can have different frequencies. Therefore Class III can offer a variety of new possibilities for the generation of resonant waves, hence, affecting the evolution of ocean wave spectrum.

For the case of normal incidence Class III Bragg resonance two examples have been studied: regular ocean wave generation as a result of nonlinear interaction of two short surface waves with a regular wavelength bottom undulation, and long infragravity wave generation via interaction of regular wavelength surface waves and bottom undulations. The latter can particularly be important in the problem of resonance of LNG carriers moored in shallow basins near the shore.

In the case of oblique resonance, it is shown that the third order Bragg resonance can generate a symmetric three dimensional standing wave pattern from a monochromatic incident surface wave via a bi-harmonic bottom topography. Oblique class III Bragg resonance is also shown to have potentials in formation of long/short surface waves oblique to the incident waves if the incident waves arrive at the bottom undulation with appropriate angles.

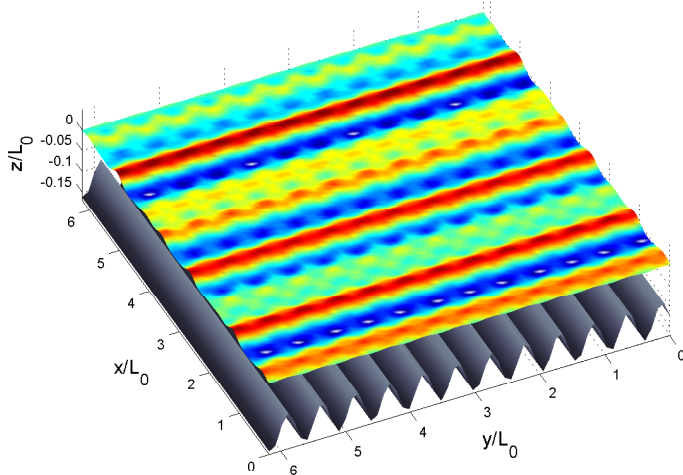
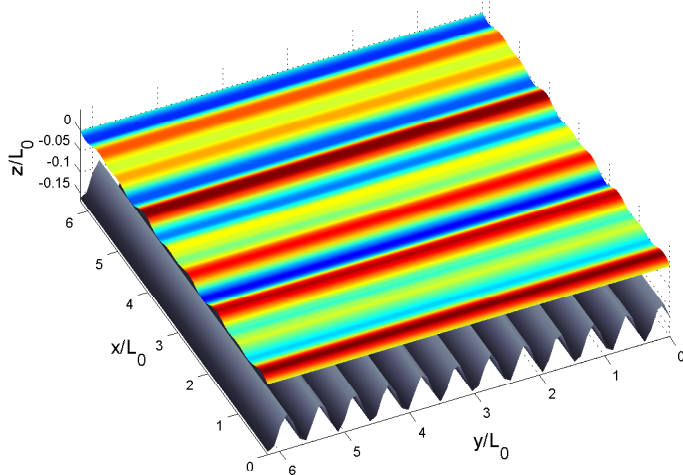


Figure 8. High order numerical simulation of waves propagating over undulatory topography when class III Bragg resonance condition is satisfied. a. Linear simulation b. higher order ($M=4$) simulation. Oblique waves $\mathbf{k}=(13, 12)$ are observed due to Class III Bragg resonance of surface waves with a perpendicular bottom undulation.

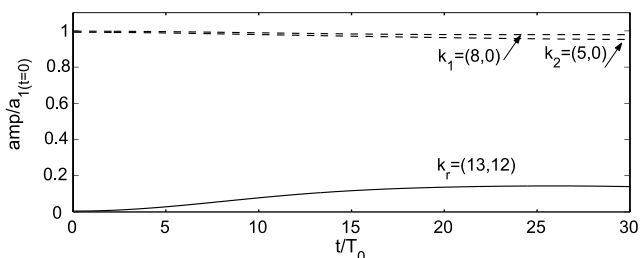


Figure 9. Evolution of amplitudes of incident and resonant waves in an oblique Class III Bragg resonance. Normalized wave numbers are shown on the figure.

Real ocean surface is composed of a spectrum of waves, so is the topography. Therefore a variety of combinations, similar to those studied in this paper, may occur resulting in an accelerated energy transfer to other frequencies. Our considerations suggest that this energy transfer, which is solely due to nonlinearity, can in fact be strong and can deform or accelerate the evolution of the ocean spectrum; therefore it has to be carefully taken into account for a safe offshore design particularly in shallow basins and near shore areas with appreciable bottom irregularities.

ACKNOWLEDGMENT

This work is funded by grants from Office of Naval Research.

REFERENCES

- [1] Mei, C. C., 1985. "Resonant reflection of surface water waves by periodic sandbars". *J. Fluid Mech.*, **152**, pp. 315–335.
- [2] Hara, T., and Mei, C., 1987. "Bragg scattering of surface waves by periodic bars: theory and experiment". *Journal of Fluid Mechanics*, **178**, pp. 221–241.
- [3] Mei, C., Hara, T., and Naciri, M., 1988. "Note on Bragg scattering of water waves by parallel bars on the seabed". *Journal of Fluid Mechanics*, **186**, pp. 147–162.
- [4] Naciri, M., and Mei, C., 1988. "Bragg scattering of water waves by a doubly periodic seabed". *Journal of Fluid Mechanics*, **192**, pp. 51–74.
- [5] Heathershaw, A. D., and Davies, A., 1985. "Resonant wave reflection by transverse bedforms and its relation to beaches and offshore bars". *Mar. Geol.*, **62**, pp. 321–338.
- [6] Renaud, M., Rezende, F., Waals, O., Chen, X., and Van Dijk, R., 2008. "Second-order wave loads on a lng carrier in multi-directional waves". In proceeding of OMAE 2008, 26th international Conference on Offshore Mechanics and Arctic Engineering, June 2008, Estoril, Portugal.
- [7] Babcock, J., Kirkendall, B., and Orcutt, J., 1994. "Relationships between ocean bottom noise and the environment". *Bulletin of the Seismological Society of America*, **84**(6), pp. 1991–2007.
- [8] Davies, A., 1982. "The reflection of wave energy by undulation on the seabed". *Dyn. Atmos. Oceans*, **6**, pp. 207–232.
- [9] Kirby, J. T., 1986. "A general wave equation for waves over rippled beds". *J. Fluid Mech.*, **162**, pp. 171–186.
- [10] Liu, Y., and Yue, D. K. P., 1998. "On generalized Bragg scattering of surface waves by bottom ripples". *J. Fluid Mech.*, **356**, pp. 297–326.
- [11] Friedrich, A., Kruger, F., and Klinge, K., 1998. "Ocean-generated microseismic noise located with the Grafenberg array". *Journal of Seismology*, **2**, pp. 47–64.

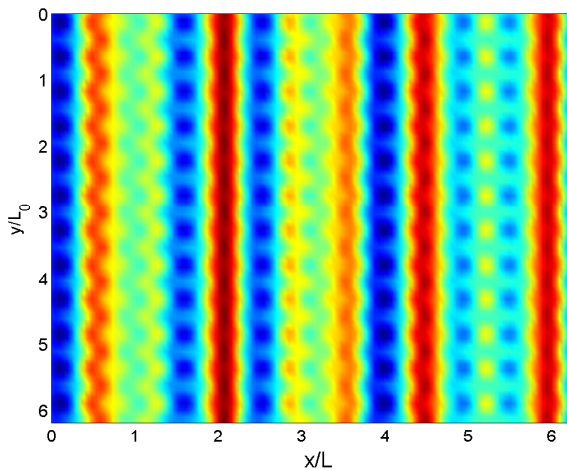
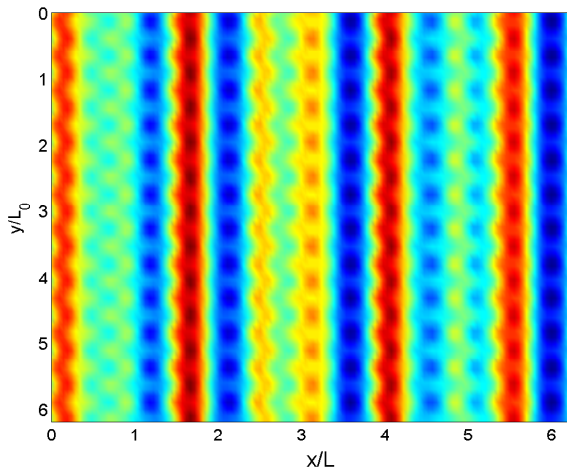


Figure 10. An evidence of double Class III Bragg resonance formation resulting in a standing wave in the y -direction. While waves are propagating in x -direction, crests and troughs are not moving in the y -direction at all. In three dimension the surface pattern looks like a moving egg-rack.

Ocean Engineering, **129**, p. 15.

- [16] van der Molen, W., and Ligteringen, H., 2005. "Influence of Loading Condition on the Behavior of a Moored Liquefied Natural Gas Ship". *Journal of Waterway, Port, Coastal, and Ocean Engineering*, **131**, p. 33.
- [17] Arduin, F., and Magne, R., 2007. "Scattering of surface gravity waves by bottom topography with a current". *J. Fluid Mech.*, **576**, pp. 235–264.
- [18] Mei, C. C., Stiassnie, M., and Yue, D. K.-P., 2005. *Theory and applications of ocean surface waves. Part 1,2*, Vol. 23 of *Advanced Series on Ocean Engineering*. World Scientific Publishing Co. Pte. Ltd., Hackensack, NJ. Linear and Nonlinear aspects.

- [12] Longuet-Higgins, M., 1950. "A Theory of the Origin of Microseisms". *Philosophical Transactions of the Royal Society of London. Series A, Mathematical and Physical Sciences (1934-1990)*, **243**(857), pp. 1–35.
- [13] Rhie, J., and Romanowicz, B., 2004. "Excitation of Earth's continuous free oscillations by atmosphere-ocean-seafloor coupling". *Nature(London)*, **431**(7008), pp. 552–556.
- [14] Guza, R., 1992. "Surface Gravity Waves And Ambient Microseismic Noise". *Technical Report. Scripps Institute of Oceanography, La Jolla, CA*.
- [15] van der Molen, W., Ligteringen, H., van der Lem, J., and de Waal, J., 2002. "Behavior of a Moored LNG Ship in Swell Waves". *Journal of Waterway, Port, Coastal, and*